



Semi-Automating Laser Vision Correction

Diego de Ortuela

Abstract

The purpose of this study is to show a semi-automated laser vision correction (LVC) with the transepithelial photorefractive keratectomy (TransPRK) surgery technique. Since more surgical steps have been automated over the years, we have standardized the TransPRK technique. We have been using it since 2010. This paper aims to illustrate the processes that are readily applicable to automation. To meet the patient's expectations and ensure that the patient has uncorrected visual acuity at least equal to the preoperative corrected vision with glasses, patient selection is crucial in refractive surgical procedures. One major benefit of automating the surgery is that it can be performed in an analogous way by each surgeon or laser correction centre, so once the standard and results are good, these can be performed by different surgeons.

Keywords: TransPRK, laser vision correction (LVC), optical coherence tomography (OCT), Support Vector Machine (SVM), refractive surgery, Myopia, photorefractive keratectomy, machine learning, AI

Introduction

The purpose of this study is to demonstrate automated laser vision correction (LVC) using the transepithelial photorefractive keratectomy (TransPRK) surgery technique. The principle of keeping it short and simple (KISS) was also found to be keeping it simple and stupid. The KISS principle states that most systems work best if they are kept simple rather than made complicated; therefore, simplicity should be a key goal in design, and unnecessary complexity should be avoided. The phrase has been associated with aircraft engineer Kelly Johnson [1]. The principle is best exemplified by the story of Johnson handing a team of design engineers a handful of tools, with the challenge that they were designing must be repairable by an average mechanic in the field under combat conditions with only these tools. Hence, the "stupid" refers to the relationship between the way things break and the sophistication available to repair them. In case of refractive surgery, we must design a simple workstation to make decisions easier for the physician and repeatable. As an accurate surgery, it will give us excellent results, resulting in satisfied patients with good vision and reducing the number of retreatments. Because more surgical steps have been automated over time, we have standardized the TransPRK technique. We have been using it since 2010. This paper aims to illustrate processes that are easily automated. The semi-automated TransPRK will be referred to the Schwind AMARIS laser platform (Schwind Eye-Tech Solutions, Kleinostheim, Germany) as a user of this platform and for virgin eyes with good visual acuity, therefore the standard case of the ophthalmology practice. One significant advantage of automating surgery is that it can be performed in an analogous manner by each surgeon or laser correction center, so once the standard and results are

Affiliation:

Aurelios Recklinghausen, 1.MD, PhD University Navarra Spain

*Corresponding author:

Diego de Ortuela, Aurelios Recklinghausen, 1. PhD University Navarra Spain.

Citation: Diego de Ortuela. Semi- Automating Laser Vision Correction. Journal of Ophthalmology and Research. 7 (2024): 42-50.

Received: August 14, 2024

Accepted: August 22, 2024

Published: August 28, 2024

satisfactory, these can be performed by different surgeons, and therefore satisfactory results can be repeated by other surgeons.

Patient selection

Refraction

When refracting, we employ a system that allows us to work semi-automated a digital phoropter, chart projectors, and an automated refractometer. The process for operating digital refractors is identical to that of manual ones; the adjustments are managed by a digital panel. All refractive data, including the glasses from the lensometer and the objective and subjective refractions, can be updated and saved to the patient's file thanks to the digital system. without any additional redundant data entry or errors in transcription. Our patient file is therefore digital. We assess astigmatism at 4 mm in diameter using the pyramidal aberrometry system Peramis (CSO-Florence, Italy) [2]. When virgin eyes are chosen for refractive surgery, this astigmatism indicates the axis and amount of astigmatism that needs to be corrected. The amount of sphere is frequently undercorrected for hyperopia and hypercorrected for myopia when the aberrometer is used. The optician uses subjective refraction to determine the quantity of sphere; in myopic eyes, this results in the least amount of negative sphere, and in hyperopic patients, it results in the most accepted sphere with a normal pupil initially and a dilated pupil later. In mydriasis, the calculated sphere represents the physiological amount that needs to be adjusted. In both physiological and mydriasis, the discrepancies between these two refractions should not be greater than 0.75 D. (dioptries). The age of the patient determines how much we can overcorrect this physiological amount. For those under 30, we use the physiological (normal pupil) sphere refraction; for those between 30 and 45, we use the mean sphere, which is the product of the dilated and normal pupil refractions; and for those 45 and beyond, we use the dilated calculated sphere. When the refraction sphere exceeds 0.75 D, we schedule a follow-up consultation to re-evaluate the minimal tolerated sphere in physiological (normal pupil).

Keratoconus Screening

Thanks to various diagnostic devices that enable us to gather accurate and detailed data, we now have advanced image tools for evaluating the cornea and the anterior morphology of the eye. We have video topography using the Placido Disc, an extremely useful unit to measure the anterior corneal shape in an accurate and reproducible manner [3]. With slit-scanning and Scheimpflug imaging, we can reconstruct the three-dimensional structure of the cornea from two-dimensional optical cross sections [4]. We can analyse the cornea thickness, posterior curvature map of the cornea, and anterior chamber depth. With the high-quality spectral domain optical coherence tomography (OCT) [5],

we get even more detailed images of the anterior segment. We obtain very high-resolution images and consequently extremely accurate and precise anatomy-topographical data related to several structures of the anterior segment: corneal epithelium, Bowman membrane, corneal stroma, corneal endothelium, posterior corneal curvature, anterior chamber, iris-sclera corneal angle, iris, pupil size and dynamics, and crystalline lens.

With MS-39 (CSO, Florence Italy) we get the combination of videokeratography Placido-disc based, and anterior segment spectral domain OCT [6], we get a detailed panorama of the anterior segment. In contrast to the Scheimpflug we get with the OCT depth information about the epithelium, so that we get precise representation as an epithelium map with a resolution of 3.6 micrometres thanks to spectral domain technology. To reduce interobserver variability or misdiagnosis we can computerize analysis using machine learning techniques [7]. Posterior corneal curvature and pachymetry data provided by Scheimpflug imaging have been investigated by Ambrosio et al [8], who showed that corneal-thickness spatial profile, corneal-volume distribution, percentage increase in thickness, and percentage increase in volume were different in keratoconic and normal eyes. Combination Placido and OCT can be automated to detect abnormal, keratoconus, suspect keratoconus, myopic post-op or normal relying on the classification by Support Vector Machine (SVM) [7], a machine learning technique screening variations against normality, and since in keratoconus such variations take place in the same position, the bulging area, to report the coincidence of the location of such variations together with corneal epithelium assessment for keratoconus detection in keratoconic eyes, epithelial thickness in the region of the cone has been reported to be thinner than that of normal eyes. We can accurately identify keratoconus and rule out eyes that are not suitable candidates for refractive surgery by using the MS-39 keratoconus screening.

Treatment plan

It should be mentioned that we are describing a treatment plan for eyes with good visual acuity and without other systemic relevant disorders that can influence the cornea. Using the ORK CAM module software, we plan the TransPRK of treatment [9] (SCHWIND eye-tech-solutions, Kleinostheim, Germany). This software serves as a planning tool for excimer laser-assisted refractive procedures. We use the AMARIS laser platform from SCHWIND eye-tech-solutions, Kleinostheim, Germany. We have a variety of correction options: the aberration-free and the customized. The aberration-free profile treats the lower-order aberrations (LOA) as spherical and cylindrical values. The customized profile uses corneal or ocular wavefront data and can treat lower and higher-order aberrations (HOA). Correcting the refractive error without causing aberrations is the aim of

our corneal surgery in virgin eyes with good visual acuity. Treatment for the vast majority of these patients involves the use of the aspheric aberration neutral "Aberration-Free" method⁹. This provides positive outcomes that do not require fixing HOA. Only spherical or cylindrical refractive values are adjusted. Moreover, the treatment does not produce significant HOA that could affect contrast vision or visual acuity. The premise behind the Aberration-Free approach is that eliminating preoperatively existing high-order aberrations is not always beneficial [10]. This is valid for eyes that achieve an important level of visual acuity without experiencing visual problems [9], which is the group of eyes in what we refer to use semi-automated LVC. Studies on untreated eyes suggest that patients with above-average visual acuity may have some degree of HOA. It was also noted that the patients with the fewest HOA were not usually the ones who had the highest visual acuities. Because the brain uses neural compensation to adapt to aberrations, the patient does not need to adjust to new visual circumstances as much.

We suggest using the ocular wavefront data from the PERAMIS system in virgin eyes. In the cases when the HOA at 6 mm is less than 0.3 μm , we only treat the LOA, which is the equivalent of treating aberration-free. That means that we filter the HOA and only treat the LOA measured by the wavefront. If the HOA at 6 mm is greater than 0.3 μm , we treat both LOA and HOA in a customized manner and therefore we cannot use the semi-automated LVC as we must tailor the treatment, treating both LOA and HOA. In most of the cases, and in these cases, we propose to use semi-automated LVC, we employ the aberration-free profile with the intention to use the ocular wavefront treatment just for treating the LOA. The benefit of using the ocular wavefront is that we can measure cyclotorsion and the astigmatism axis using the same instrument, the aberrometer PERAMIS, and export this data as one file. Since we have the PERAMIS pyramidal aberrometer, we have noticed that the astigmatism axis, measured at 4 mm, is the most accepted astigmatism in the subjective refraction. We prefer to utilize PERAMIS's computed objective cylinder and the same data for the cyclorotation. Prior to starting the laser treatment, we measure the static cyclorotation between the supine position under the laser and the seated position measured with the PERAMIS aberrometer using an infrared camera. This measurement is performed right before treatment starts, unlike with other refractive intrastromal or intralamellar surgeries. Numerous studies have computed the impact of cyclotorsion during laser treatment [11-13] showing the refractive error with incorrect cyclotorsion compensation. Additionally, it is possible to select and place the center of the treatment objectively. We employ the Videokeratography information in our case [14]. With the MS-39 we have an instrument with combination of Placido disc and OCT. The Vertex center, or the center of the rings, is obtained from the Placido disc [14, 15] and we utilize

this geometrical point as the treatment's center and point of reference. The offset is the distance between the pupil center and the vertex of the cornea. We use the full offset and treat the LOA. Some authors use 2/3 of the offset [16]. We also have two different ablation strategies: the symmetric strategy with a concentric treatment with the vertex and the asymmetrical strategy where the treatment is concentric to the pupil, but the center is the vert. ex of the cornea, by doing this, tissue is spared from the need to increase the optical zone. Since the TransPRK allows us to increase the optical zone, we prefer the symmetrical approach [17] because the postoperative topography shows greater symmetry. We advise using an optical zone that is at least twice the offset distance in addition to the pupil in mesopic for the minimum optical zone. Since the software can now extend the treatment by 1 mm from the measurement of the aberrometry, we should attempt to measure with the aberrometer under mesopic conditions and with a large pupil. The ORK-CAM also computes the minimal optical zone (OZ). The transition zone is also computed by the software using the optical zone and refraction as inputs. So, we get in one file from the OW the refraction, the infrared photography for static cyclotorsion, the LOA are treated, and the HOA are filtered getting the same profile as aberration-free. From the placido rings, we get: the position of the vertex in relation to the limbus and pupil; the keratometry values; from the OCT, the epithelium thickness at the center and the mean thickness at a 4 mm radius; the total pachymetry; and the standard optical zone of 6.7 mm (which is our standard), which can be changed to a bigger OZ if needed; the transition zone is calculated by the software.

Laser Platform

We use of the SCHWIND AMARIS 1500Hz RS laser, which has a Super-Gaussian beam profile and a small 0.54-millimetre spot size using two fluences the higher fluence with 500mj/cm² and the low fluence with 300mj/cm² (SCHWIND eye-tech-solutions, Kleinhostheim, Germany). The improved spot overlap matrix prevents vacancies and corneal roughness by an accurate reproduction of the computed ablation volume. The system can shorten the ablation time while keeping the same tissue conditions throughout thanks to the 1050 Hz ablation's high speed. The Intelligent Thermal Effect Control (ITEC) on the SCHWIND AMARIS laser systems guards against damage to the surrounding corneal tissue even at extremely high ablation speeds. The ITEC algorithm [18] distributes the laser pulses in a way that is both thermally optimized and dynamically adjusted, allowing the cornea to cool down sufficiently. This enables faster approach of a position that has already cooled by subsequent pulses. Our in vivo thermal measurements²³ demonstrate that the cornea's temperature rise is always significantly less than 40°, which is thought to be critical for corneal tissue denaturation and is never greater than 5°. The laser systems actively compensate for

eye movements with an average latency of about 1.6 ms. An integrated eye tracker monitors the eye's position 1,050 times per second. The camera, scanner, electronics, and software all work together to provide an overall reaction time for the AMARIS that is typically less than 3 ms. The precision with which the laser spots are positioned, and the eye is centred determine the accuracy of the results of a refractive treatment [19]. Apart from the pupil, the limbus is also detected by the eye tracker. Unlike the pupil's diameter, the limbus's size is constant. Because of this, the limbus is used as a reference for ablation, preserving the original ablation centre throughout the course of treatment. This enables us to select the exact location of the ablation centre in our case the vertex of the cornea, which stays in that position the entire time because the laser system tracks the movement of the pupil in relation to the limbus. Automatic pupil size monitoring during static cyclotorsion control provides extra security [12]. To maintain the same pupil size at the beginning of treatment as it did during the preoperative exam, which is when the diagnostic data was gathered, the lighting is automatically adjusted. During ablation, changes in corneal curvature combined with a non-normal laser beam incidence result in efficiency and reflection losses [20]. By taking these losses into account, the ORK-CAM software makes sure that the necessary ablation volume is accurately removed. As a necessary result, the patient's refractive deficit and the keratometry readings for both meridians are imported from the video keratography into the ORK-CAM software at the proper vertex distance.

Pearl – TransPRK

Transepithelial Photorefractive Keratectomy (TransPRK), a no-touch, all-laser surface ablation, is an advanced method of surface treatments [21, 22]. The laser system thus ablates the regenerating surface of the eye, the epithelium, and then the stroma. When using the TransPRK, treating an eye's surface does not require touching the eye with an instrument. The ORK-CAM includes distinct tissue ablations for the stroma and the epithelium [23] in the computation to avoid unintended refractive effects during epithelium ablation. Because the epithelium is known to be thicker in the periphery, the software in standard modus ablates with a central diameter of 55 μm and a peripheral diameter of 65 μm , or 8.0 mm. As we are now able to precisely measure the epithelium we can carry out a customized epithelium treatment with the MS-39 (CSO, Florence, Italy) [24]. We import the data of the central epithelium as well as the mean epithelium thickness at 8 mm of diameter. In a customized way, the software ablates this imported amount, considering that at the periphery we have a loss of energy. A small deviation from this averaged value of epithelial thickness will not lead to an over- or under-correction; instead, a thinner or thicker epithelium will result in a slightly deeper ablation or a smaller optical zone [25]. In both situations, the desired

refractive change and curvature shape will be achieved. Directly beneath the area where the epithelium is removed by laser is the total zone of ablation (TZ), which is the total of the transition zone and the chosen optical zone (OZ) (TZ). Due to the smaller wound surface compared to manual PRK, the healing process takes one or two days less [26]. When we consider lesser amounts of refractive error as being under two dioptres of myopia [25], this becomes especially interesting. In addition, a single procedure is used to ablate both the stroma and the epithelium. This significantly reduces the total amount of time needed for treatment and diminishes the possibility of corneal dehydration [27].

Material

To demonstrate that semi-automated TransPRK gives satisfactory results in virgin eyes with good visual acuity at least 0.8 Snellen acuity and less than 0.3 micron of HOA at 6 mm, we performed a retrospective study of a consecutive group of myopic eyes treated in Aurelios Recklinghausen, Germany, with at least a follow-up of 3 months. The mean preoperatively spherical equivalent was -3.52 dioptres (D) with a range between -0.75D and -7D and a mean preoperatively astigmatism of 0.98D with a range of -2.75D. In all the cases, the same surgeon, DdO, treated with TransPRK. As all the cases had good visual acuity, we treated with the aberration-free profile. As described before, we created one file of a patient under the automated phoropter. The measured astigmatism by the PERAMIS was imported, and the optician calibrated the sphere as described. The file of the aberrometry from the PERAMIS was exported after adjusting the sphere as measured by the optician. From this file of ocular aberrometry, we filtered the HOA to treat only the LOA (sphere and cylinder). With this file, we also got the cyclotorsion information for the laser platform to adjust the static cyclotorsion of the eye from sitting to supine position. From the MS-39, we had a second file. Here we get information on the keratometry, the position of the vertex of the cornea in relation to the limbus, the central pachymetry, and the epithelial map with the mean centre thickness and the mean peripheral thickness. The MS-39 also has software to calculate if the patient has a normal cornea or if keratoconus is suspected, and therefore exclude abnormal eyes. With these files, we get one ORK CAM file (see figure 1-3). In this case, the software also calculates if the residual stroma is enough (at least 250 μm). With this file, we begin the treatment under the laser. After the calibration, we use infrared photography to identify the eye. If we have the correct patient, the software will recognize the eye and correct the static cyclotorsion. After that, the ablation occurs in these cases between 22 seconds and 59 seconds, depending on the refractive error. The results in this group of eyes were exceptionally good, with a postoperative SEQ of -0.02D and a mean postoperative cylinder of -0.11D. For more details, see Table 1.

Table 1:

N=65 eyes				
Gender	female	66.2% (43 eyes)	male	33.8% (22 eyes)
eye	left	50.8% (33 eyes)	right	49.2% (32 eyes)
	Preoperatively	range	Postop 3 m	range
SEQ	-3.52 D +/- 1.67D	(-0.75 to -7D)	-0.02 D +/- 0.26 D	-0.63 D to +0.75D
Sphere	-3.03 D +/- 1.7D	(-0.5 to -6.75D)	+0.03 D +/- 0.23D	-0.5D to +0.75D
Cyl	-0.98 D +/- 0.74 D	(0 to -2.75D)	-0.11D +/- 0.18D	-0.75 D to 0D

Demographic data with spherical equivalent (SEQ), sphere, Cylinder (Cyl) in dioptres D showing mean and standard deviation.

The screenshot displays the SCHWIND eye-tech-solutions software interface. At the top, patient information is entered: Patient-ID: P2078403669, Date of birth: 11/04/1978, Age: 44, Last name: [redacted], First name: [redacted], Gender: Female, and Comment: [redacted]. The interface is divided into several sections. The 'Refraction' section shows 'ow' (Ocular Wave) and 'OD' (Right Eye) data. It includes fields for 'Refract' (VD: 12.0 mm), 'Manifest' (Sphere: -2.76, Cylinder: -1.72, Axis: 1), 'Target' (Sphere: 0.00, Cylinder: 0.00, Axis: 1), and 'Laser' (Sphere: -2.76, Cylinder: -1.72, Axis: 1). A 'Compound Myopic Astigmatism' banner is present. The 'Keratometry' section shows 'Pre-Op' (K1: 43.62, K2: 45.49, Average K: 44.55) and 'Target (estimated)' (K1: 41.09, K2: 42.01, Average K: 41.55). The 'Wavefront info' section shows 'Import diameter: 5.24 mm', 'ext. Zernike refraction @ 4.00 mm pupil Ø: -2.76 -1.72 X 1 @ VD = 12.0 mm', 'Pupil Offset: Ø: 2.95 mm / R: 0.25 mm @ 103 °', and 'Imported file: fi_p2078403669_19781104_od_2023073115130'. The 'SCC info' section shows 'SCC device: SCHWIND PERAMIS', 'Status: Data quality OK', and 'Imported file: p2078403669_19781104_od_2023073115130'. At the bottom, there are buttons for 'TransPRK', 'PRK', 'LASEK', 'LASIK', 'FemtoLASIK', 'Re-Lift', 'OK', 'Cancel', and 'Keyboard on'.

Figure 1: created file with the ORK-CAM software. The patient has one number that is also identical to the imported files. Using the aberrometer, we were able to obtain the refraction and the statistical cyclotorsion (SCC). Additionally from the anterior segment OCT we obtained the keratometry data, the epithelium thickness, and the pupil offset for the centration.

No one loses more than one line of corrected distance visual acuity. The refractive outcome was in 95% of the cases under 0.5D and 100% of the cases under 1D. The refractive astigmatism was in 98% of the cases under 0.5D and in 100% of the cases under 1D. The predictability was

particularly good, with a coefficient of regression of 0.98, which is close to one, showing excellent predictability. The average deviation from the attempted versus achieved SEQ was -0.03 D. Further details are shown in figure 4-6.

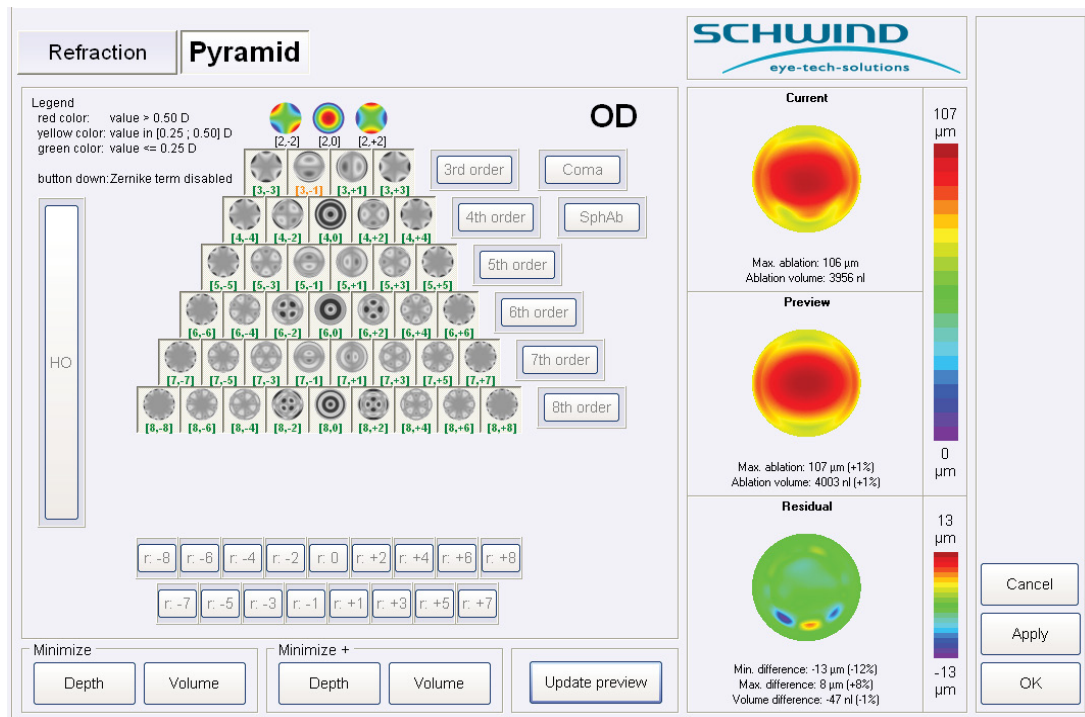


Figure 2: From the aberrometry, we get information on the lower-order aberrations (LOA) and the higher-order aberrations (HOA). As we treat in virgin eyes with good visual acuity only the LOA we filter the HOA. At the right top is the profile with HOA and LOA; in the right middle is the treatment of the LOA; and at the right bottom is the residual untreated HOA.



Figure 3: The ablation profile map that is imported to the laser platform. The optical zone (OZ) and the transition zone (TZ) are calculated based on the measurement in mesopic conditions of the Peramis aberrometry. Residual thickness is also shown.

Refractive outcome - Percentage within Attempted

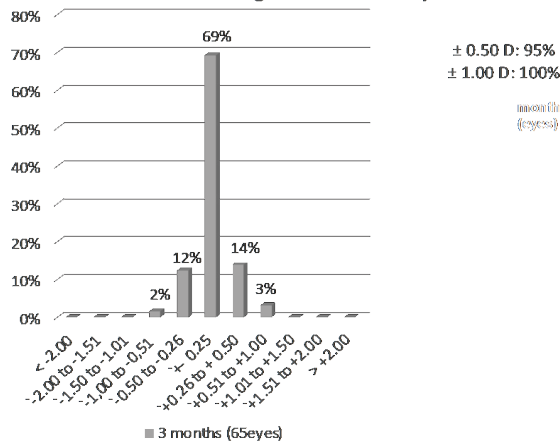


Figure 4: Refractive outcome in spherical equivalent (SEQ) after 3 months of the TransPRK treatment.

Change in CDVA - Percentage 'SAFETY'

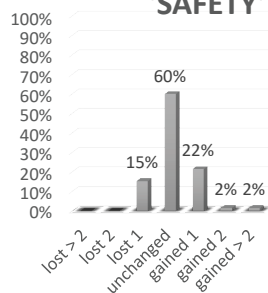


Figure 5: Safety of the TransPRK procedure. No eye loose 2 or more lines of Snellen vision.

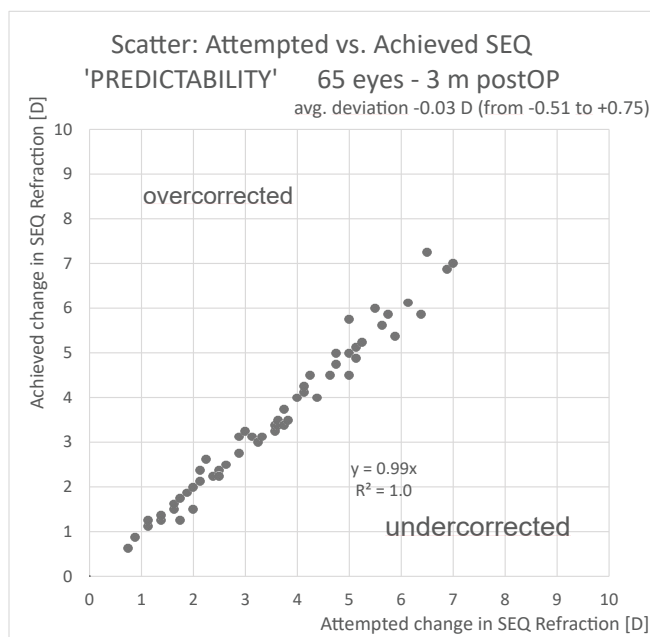


Figure 6: Predictability showing attempted correction versus achieved correction. The regression coefficient y is near to 1, showing a good predictability.

Discussion

When it comes to refractive surgery, it is essential to screen candidates before they undergo corneal refractive surgery to avoid complications. We have tools and screening methods that utilize machine learning techniques [28–30] to determine whether corneal refractive surgery is appropriate for the patient. Using digital workflows, we are also able to obtain more accurate and reliable measurements of refractive errors [31]. Our recommendation also includes the utilization of a single digital file for each individual patient, with the objective of minimizing the number of transcription errors. With the help of the aberrometry, topography and anterior OCT we can screen eyes with good visual acuity and exclude the need of treatment of HOA and therefore use the LOA from the aberrometry. We as doctors must decide if the treatment is a standard treatment in these case aberration-free and if not if we need to use corneal data or ocular data for a wavefront treatment. That's why the described treatment is semi-automated. Once we have decided if the eye is normal, we can use the proposed schema.

We suggest a simplified way to treat refractive errors with advanced surface ablation TransPRK. We have shown that a most of the processes can be automated as astigmatism from the Aberrometer. Other authors also propose to use the data of the aberrometry but then using a nomogram [32], we have found that this is not necessary with the pyramidal aberrometer. The pyramidal aberrometer shows 0.2D of repeatability for astigmatism measured at 5mm of pupil diameter [33]. Comparing pyramidal aberrometry to Hartmann-Shack aberrometry, there are theoretical advantages in terms of higher dynamic range and higher sampling density [33]. Furthermore, it is suggested that the optometrist should only have control over the sphere; the patient's age determines how much we overcorrect this physiological amount. The physiological pupil sphere refraction is used for individuals under 30, the mean sphere, which is the product of the dilated and normal pupil refractions, is used for individuals between 30 and 45, and the dilated calculated sphere is used for individuals 45 and over. The decision of which kind of treatment Aberration-free, Ocular wavefront or Corneal wavefront (topographic guided) must be done by the surgeon, in most of the cases in virgin eyes we can use the aberration-free or in a similar way the OW filtering the aberrations and treating only the LOA with allows us to get an automated file. In cases of complication, we must decide per case, and this cannot be completely automated as the surgeon is the responsible and not the laser system. But in the standard case of virgin eyes, we have shown that a lot of data is created in one file and imported before the treatment, allowing us to perform a semi-automated surgery. This data is imported together with the MS-39 data that gives us the epithelium thickness at the centre and at the periphery, the pachymetry data, the keratometry data, the cyclotorsion data as limbus and pupil

centre and the position of the vertex in relation to these two geometrical data. We have obtained with this semi-automated technique at least results that are comparable to those that have been published in the past. The effectiveness and safety of the TransPRK procedures have been extensively demonstrated to be a successful technique for treating myopia and myopic astigmatism [21,34–38]. Limitations of this study include the non-comparative nature of the study and its utilization of prior research to evaluate findings pertaining to measurement repeatability in relation to manifest refraction and treatment outcomes. As a result, we are unable to address potential benefits for subjective visual outcomes between aberrometry guided semi-automated TransPRK and traditional TransPRK treatment. And that only standard normal eyes can use the semi-automated surgery.

Conclusion

We have introduced a standard for normal eyes with good visual acuity procedure that automates refractive surgery with TransPRK using the Aberrometry for the refraction (LOA). From the anterior OCT and videokeratography, we export the data for centration, keratometry reading, epithelium thickness, and cyclotorsion. All these measurements are imported into a file, which enables them to be treated automatically.

Funding: This research received no external funding.

Institutional Review Board Statement: The study did not require ethical approval as it is retrospective.

References

1. The Minneapolis Star. Published online February 12 (1938).
2. Singh NK, Jaskulski M, Ramasubramanian V, et al. Validation of a Clinical Aberrometer Using Pyramidal Wavefront Sensing. *Optom Vis Sci* 96 (2019): 733-744.
3. Liu Z, Huang AJ, Pflugfelder SC. Evaluation of corneal thickness and topography in normal eyes using the Orbscan corneal topography system. *Br J Ophthalmol* 83 (1999): 774-778.
4. Konstantopoulos A, Hossain P, Anderson DF. Recent advances in ophthalmic anterior segment imaging: a new era for ophthalmic diagnosis? *Br J Ophthalmol* 91 (2007): 551-557.
5. Li Y, Meisler DM, Tang M, et al. Keratoconus diagnosis with optical coherence tomography pachymetry mapping. *Ophthalmology* 115 (2008): 2159-2166.
6. Savini G, Schiano-Lomoriello D, Hoffer KJ. Repeatability of automatic measurements by a new anterior segment optical coherence tomographer combined with Placido topography and agreement with 2 Scheimpflug cameras. *Journal of Cataract & Refractive Surgery* 44 (2018).
7. Arbelaez MC, Versaci F, Vestri G, Barboni P, Savini G. Use of a Support Vector Machine for Keratoconus and Subclinical Keratoconus Detection by Topographic and Tomographic Data. *Ophthalmology* 119 (2012): 2231-2238.
8. Luz A, Lopes B, Salomão M, Ambrósio R. Application of corneal tomography before keratorefractive procedure for laser vision correction. *J Biophotonics* 9 (2016): 445-453.
9. Arba-Mosquera S, de Ortueta D. Analysis of optimized profiles for “aberration-free” refractive surgery. *Ophthalmic Physiol Opt* 29 (2009): 535-548.
10. Artal P, Chen L, Fernández EJ, Singer B, Manzanera S, Williams DR. Neural compensation for the eye’s optical aberrations. *Journal of Vision* 4 (2004): 4.
11. Adib-Moghaddam S, Soleyman-Jahi S, Tofighi S, et al. Factors Associated With Ocular Cyclotorsion Detected by High-Speed Dual-Detection Eye Tracker During Single-Step Transepithelial Photorefractive Keratectomy. *J Refract Surg* 34 (2018): 736-744.
12. Arba-Mosquera S, Merayo-Llodes J, de Ortueta D. Clinical effects of pure cyclotorsional errors during refractive surgery. *Invest Ophthalmol Vis Sci* 49 (2008): 4828-4836.
13. Arba-Mosquera S, Aslanides IM. Analysis of the effects of Eye-Tracker performance on the pulse positioning errors during refractive surgery. *Journal of Optometry* 5 (2012): 31-37.
14. de Ortueta D, Schreyger FD. Centration on the cornea vertex normal during hyperopic refractive photoablation using videokeratoscopy. *J Refract Surg* 23 (2007): 198-200.
15. Mosquera SA, Verma S, McAlinden C. Centration axis in refractive surgery. *Eye and Vis* 2 (2015): 4.
16. Kermani O. Automated visual axis alignment for refractive excimer laser ablation. *J Refract Surg* 22 (2006): S1089-1092.
17. De Ortueta D, Von Rüdén D, Arba Mosquera S. Symmetric offset versus asymmetric offset ablation with transepithelial refractive keratectomy. *BMC Ophthalmol* 23 (2023): 219.
18. Brunsman U, Sauer U, Dressler K, Triefenbach N, Mosquera SA. Minimisation of the thermal load of the ablation in high-speed laser corneal refractive surgery: the ‘intelligent thermal effect control’ of the AMARIS platform. *null* 57 (2010): 466-479.
19. Arba-Mosquera S, Hollerbach T. Ablation Resolution in Laser Corneal Refractive Surgery: The Dual Fluence Concept of the AMARIS Platform. *Advances in Optical Technologies* (2010): 1-13.

20. Arba-Mosquera S, de Ortueta D. Geometrical analysis of the loss of ablation efficiency at non-normal incidence. *Opt Express* 16 (2008): 3877-3895.
21. Aslanides IM, Kymionis GD. Trans advanced surface laser ablation (TransPRK) outcomes using SmartPulseTechnology. *Cont Lens Anterior Eye* 40 (2017): 42-46.
22. Aslanides IM, Padroni S, Arba Mosquera S, Ioannides A, Mukherjee A. Comparison of single-step reverse transepithelial all-surface laser ablation (ASLA) to alcohol-assisted photorefractive keratectomy. *Clin Ophthalmol* 6 (2012): 973-980.
23. Seiler T, Kriegerowski M, Schnoy N, Bende T. Ablation rate of human corneal epithelium and Bowman's layer with the excimer laser (193 nm). *Refract Corneal Surg* 6 (1990): 99-102.
24. de Ortueta D, von Rüdén D, Arba-Mosquera S. Customized versus Standard Epithelium Profiles in Transepithelial Photorefractive Keratectomy. *Optics* 2 (2021): 266-275.
25. de Ortueta D, von Rüdén D, Arba-Mosquera S. Comparison of Refractive and Visual Outcomes after Transepithelial Photorefractive Keratectomy (TransPRK) in Low versus Moderate Myopia. *Photonics* 8 (2021): 262.
26. Lee HK, Lee KS, Kim JK, Kim HC, Seo KR, Kim EK. Epithelial healing and clinical outcomes in excimer laser photorefractive surgery following three epithelial removal techniques: mechanical, alcohol, and excimer laser. *Am J Ophthalmol* 139 (2005): 56-63.
27. de Ortueta D, von Rüdén D, Magnago T, Arba Mosquera S. Influence of stromal refractive index and hydration on corneal laser refractive surgery. *J Cataract Refract Surg* 40 (2014): 897-904.
28. Yoo TK, Ryu IH, Lee G, et al. Adopting machine learning to automatically identify candidate patients for corneal refractive surgery. *npj Digit Med* 2 (2019): 59.
29. Ting DSW, Pasquale LR, Peng L, et al. Artificial intelligence and deep learning in ophthalmology. *Br J Ophthalmol* 103 (2019): 167-175.
30. Ang M, Gatineau D, Reinstein DZ, Mertens E, Alió Del Barrio JL, Alió JL. Refractive surgery beyond 2020. *Eye* 35 (2021): 362-382.
31. Ohlendorf A, Leube A, Wahl S. Advancing Digital Workflows for Refractive Error Measurements. *JCM* 9 (2020): 2205.
32. Allan BD, Hassan H, Jeong A. Multiple regression analysis in nomogram development for myopic wavefront laser in situ keratomileusis: Improving astigmatic outcomes. *Journal of Cataract and Refractive Surgery* 41 (2015): 1009-1017.
33. Frings A, Hassan H, Allan BD. Pyramidal Aberrometry in Wavefront-Guided Myopic LASIK. *J Refract Surg* 36 (2020): 442-448.
34. Kaluzny BJ, Cieslinska I, Mosquera SA, Verma S. Single-Step Transepithelial PRK vs Alcohol-Assisted PRK in Myopia and Compound Myopic Astigmatism Correction. *Medicine (Baltimore)* 95 (2016): e1993.
35. Antonios R, Abdul Fattah M, Arba Mosquera S, Abiad BH, Sleiman K, Awwad ST. Single-step transepithelial versus alcohol-assisted photorefractive keratectomy in the treatment of high myopia: a comparative evaluation over 12 months. *Br J Ophthalmol* 101 (2017): 1106-1112.
36. de Ortueta D, von Rüdén D, Verma S, Magnago T, Arba-Mosquera S. Transepithelial Photorefractive Keratectomy in Moderate to High Astigmatism with a Non-wavefront-Guided Aberration-Neutral Ablation Profile. *J Refract Surg* 34 (2018): 466-474.
37. Adib-Moghaddam S, Soleyman-Jahi S, Sanjari Moghaddam A, et al. Efficacy and safety of transepithelial photorefractive keratectomy. *J Cataract Refract Surg* 44 (2018): 1267-1279.
38. Fadlallah A, Fahed D, Khalil K, et al. Transepithelial photorefractive keratectomy: clinical results. *J Cataract Refract Surg* 37 (2011): 1852-1857.